THE ASTROPHYSICAL JOURNAL, 308:765–780, 1986 September 15

X-RAY AND OPTICAL OBSERVATIONS OF THE ULTRASHORT PERIOD DWARF NOVA SW URSAE MAJORIS: A LIKELY NEW DQ HERCULIS STAR

A. W. SHAFTER
McDonald Observatory and Department of Astronomy, University of Texas at Austin
P. SZKODY[1, 2]
Department of Astronomy, University of Washington
AND
J. R. THORSTENSEN
Department of Physics and Astronomy, Dartmouth College
Received 1985 October 21; accepted 1986 February 24

ABSTRACT

Optical photometric and spectroscopic and X-ray observations of the dwarf nova SW UMa are presented. Moderate resolution spectroscopic data have established an orbital period of 81.8 minutes and have revealed that the Balmer emission lines have a multiple structure. A narrow component, similar to the s-wave component which is sometimes seen in cataclysmic variables, has been identified in SW UMa. The phasing of this component suggests, however, that the source of the emission cannot be the hot spot where the interstar mass transfer stream impacts the disk. Nor can it be associated with accreting magnetic poles of a rapidly rotating white dwarf because of its orbital phase stability. The narrow component is almost in phase with the Balmer line wings, implying that the emission arises in a region of the disk facing away from the white dwarf. In particular, accretion disk models with nonaxisymmetric line emission have been computed which allow us to isolate the location of the excess emission to a region of the disk which is essentially opposite to where the hot spot is expected to be found.

Photometric observations have revealed the presence of a hump in the light curve occurring at an orbital phase which is consistent with the phase at which the region of enhanced line emission is most favorably seen ($\phi = 0.3$). Changes in the hump amplitude are seen from night to night and a 15.9 minute periodicity is evident in the light curve. Low-energy (0.05–2 keV) *EXOSAT* observations show identical orbital and 15.9 minute modulations, thus linking the optical and X-ray continuum and the excess line emission to the same region. The presence of the 15.9 minute optical and X-ray periodicities suggest that SW UMa, in addition to being a dwarf nova, is also a member of the DQ Her class of cataclysmic variables. At 81.8 minutes, SW UMa has the shortest orbital period of any DQ Her system and one of only two such systems below the period gap (the other being EX Hya).

Subject headings: stars: binaries — stars: dwarf novae — stars: individual — stars: X-rays — X-rays: binaries

I. INTRODUCTION

Cataclysmic binaries are systems consisting of a white dwarf (the primary) which accretes material from a Roche-lobe–filling red dwarf companion (the secondary). In order to conserve angular momentum, the transferred material usually forms a ring encircling the white dwarf. Viscous stresses rob the material in the ring of its angluar momentum, causing the ring to spread out into a disk. Eventually the material accretes onto the equatorial region of the white dwarf. The resulting release of gravitational potential energy heats the disk, typically making it the dominant source of optical and UV radiation in the system. (For general reviews of cataclysmic variables see Robinson 1976; Warner 1976; and Wade and Ward 1985).

In cases where the white dwarf has a sufficiently strong magnetic field the inner regions of the accretion disk may be disrupted or, for even stronger fields, the disk may not form at all. Systems falling into the former category are called DQ Her systems or intermediate polars (Lamb 1983; Warner 1983). In these systems the material becomes trapped by the magnetic field lines in the inner regions of the accretion disk and accretes onto the magnetic poles of the white dwarf. As a result of heating caused by accretion onto the magnetic poles, the DQ Her stars are characterized by optical and X-ray modulations at the rotation period of the white dwarf. Because the magnetic field is not strong enough to lock the white dwarf into synchronous rotation with the binary, the white dwarfs in DQ Her systems have rotation periods which are typically one or two orders of magnitude shorter than the orbital period.[3] Reflection effects in the system usually produce a photometric modulation at the beat period between the white dwarf rotation period and the orbital period. Systems where the magnetic field is sufficiently strong to lock the white dwarf into synchronism are known as AM Her systems. Excellent descriptions of AM Her systems can be found in reviews by Liebert and Stockman (1985) and Chiapetti, Tanzi, and Treves (1980).

[1] Visiting Astronomer, KPNO, NOAO, operated by AURA, Inc., under contract with the NSF.
[2] Visiting Astronomer, *EXOSAT* satellite.
[3] The term "intermediate polar" is usually reserved to describe systems with relatively long white dwarf rotation periods (~ 1000 s). Such systems are also referred to as long-period DQ Her stars (Penning 1985). For the sake of simplicity, we will refer to all such systems as DQ Her stars.

In systems containing an accretion disk (i.e., non–AM Her systems), a shock front or "hot spot" is usually formed near the point where the interstar mass transfer stream impacts the disk. In many systems the hot spot is a significant source of continuum and line emission. Probably the best example of such a system is the well-known dwarf nova, U Gem (Stover 1981; Smak 1971, 1976). The hot spot in U Gem produces a strong orbital modulation (hump) in the light curve peaking near $\phi = 0.8$, as demonstrated by Warner and Nather (1971). This phase is consistent with the hump being caused by the changing aspect of the impact point of the stream and the disk.

In addition to being a source of continuum emission, the hot spot is typically a source of line emission as well. Radial velocity studies of U Gem (Stover 1981; Smak 1976) have revealed a relatively narrow emission line component with a velocity amplitude of several hundred km s^{-1}. This component is usually referred to as the "s-wave" component because it appears to form an s-shaped figure on single-trailed spectrograms. The radial velocity studies of Smak and Stover have demonstrated that the radial velocity of the s-wave component in U Gem has a zero crossing at the orbital phase where the hump in the light curve occurs. They conclude that the phasing of the s-wave component can be simply explained if this component reflects the velocity of the interstar mass transfer stream or of the disk material at the location of the hot spot.

A considerable body of evidence has been building lately which indicates that the simple hot-spot model outlined above is inadequate to describe the photometric and spectroscopic properties of a significant fraction of cataclysmic variables. For example, Schlegel, Honeycutt, and Kaitchuk (1983) and Kaitchuck, Honeycutt, and Schlegel (1983) have found that s-wave components in UX UMa and RW Tri appear to be almost precisely 180° out of phase with the white dwarf. They conclude that the s-wave components seen in these two systems are hard to explain as arising from a canonical hot-spot. Even more surprisingly, Shafter and Szkody (1984) found that the phasing of the s-wave component seen in the ultrashort period dwarf nova T Leo lagged that of the white dwarf by more than 180°. If the s-wave component observed in T Leo is assumed to arise at the location where the interstar mass transfer stream impacts the disk, then the stream would have to impact on the leading side of the disk!

In this paper we report time-resolved X-ray and optical photometric, and optical spectroscopic observations of the ultrashort period cataclysmic variable SW UMa. The optical and X-ray light curves presented here suggest the SW UMa is a member of the DQ Her class of cataclysmic variable. This is of considerable interest for two reasons. First, SW UMa has the shortest orbital period of any known DQ Her system. Indeed, only one other DQ Her system, EX Hya, has an orbital period below the 2–3 hr gap in the period distribution of cataclysmic variables. Second, SW UMa has exhibited dwarf nova eruptions with an amplitude of ~5 mag (Williams 1983). EX Hya has also been observed to have dwarf-nova type eruptions, but of a lower amplitude.

Our Spectroscopic observations of SW UMa reveal the presence of an s-wave component which is almost in phase with the extreme line wings and presumably the white dwarf! This very unusual phasing in conjunction with the available optical and X-ray data seem to indicate that a region of enhanced emission exists on the *opposite* side of the disk from the expected location of the hot spot.

II. OBSERVATIONS

a) Spectroscopy

The spectroscopic observations presented here were obtained with the image dissector scanner at Mount Lemmon Observatory and with the photon-counting, intensified reticon spectrograph at McGraw-Hill Observatory. The Mount Lemmon scanner is a copy of the original Lick Observatory image tube scanner (Robinson and Wampler 1972). The McGraw-Hill reticon is an improved version of the one described by Shectman and Hiltner (1976). The Mount Lemmon scanner was mounted at the Cassegrain focus of the University of California, San Diego/University of Minnesota 1.52 m reflector and the McGraw-Hill reticon was used at the Cassegrain focus of the 1.3 m telescope.

The Mount Lemmon data consist of both high- and low-resolution observations. The low-resolution data were obtained by using a 600 lines mm^{-1} grating in first order. This grating yielded a useful spectral range of 3800–7000 Å at a resolution of ~11 Å FWHM. Our low-resolution spectrum is presented in Figure 1. The spectrum appears to be similar to another ultrashort period system T Leo (Shafter and Szkody 1984). Low dispersion spectra of both systems show a hint of broad absorption at Hβ and possibly Hγ similar to the spectrum of the well-known ultrashort period dwarf nova WZ Sge. The broad absorption seen in T Leo and SW UMa is almost certainly produced in the photosphere of the white dwarf because both systems appear to have relatively low mass accretion rates. Disk absorption is expected to be seen only in systems with relatively high mass accretion rates and optically thick disks such as dwarf novae in eruption. The equivalent widths of the principal emission lines for SW UMa are presented in Table 1. The equivalent widths for T Leo and another ultrashort period dwarf nova, VW Vul (Shafter 1985*a*) are shown for comparison.

In addition to the low-resolution observations, we obtained a series of higher resolution observations for the radial velocity study. The Mount Lemmon data were obtained during the night of 1982 December 27 UT and during three consecutive nights the following February (1983 February 11–13 UT). The four nights yielded a total of 81 eight-minute spectra covering a 1200 Å region centered on Hα. These data were obtained with a 1200 lines mm^{-1} grating in first order and have a spectral resolution of ~4 Å.

The McGraw-Hill radial velocity data have a resolution of ~5.5 Å and also cover Hα. These data were obtained simulta-

TABLE 1

EQUIVALENT WIDTHS OF THE PRINCIPLE OPTICAL EMISSION LINES OF SW UMA AND OF TWO SIMILAR ULTRASHORT PERIOD CATACLYSMIC VARIABLES

	EQUIVALENT WIDTH (Å)		
LINE	SW UMa	T Leo	VW Vul
Hδ	21	35	61
Hγ	37	37	81
He I λ4471	5	8	22
Hβ	52	62	114
He I λ4922	4	3	9
He I λ5015	6	5	6
He I λ5876	15	20	35
Hα	138	87	144
He I λ6678	8	8	18

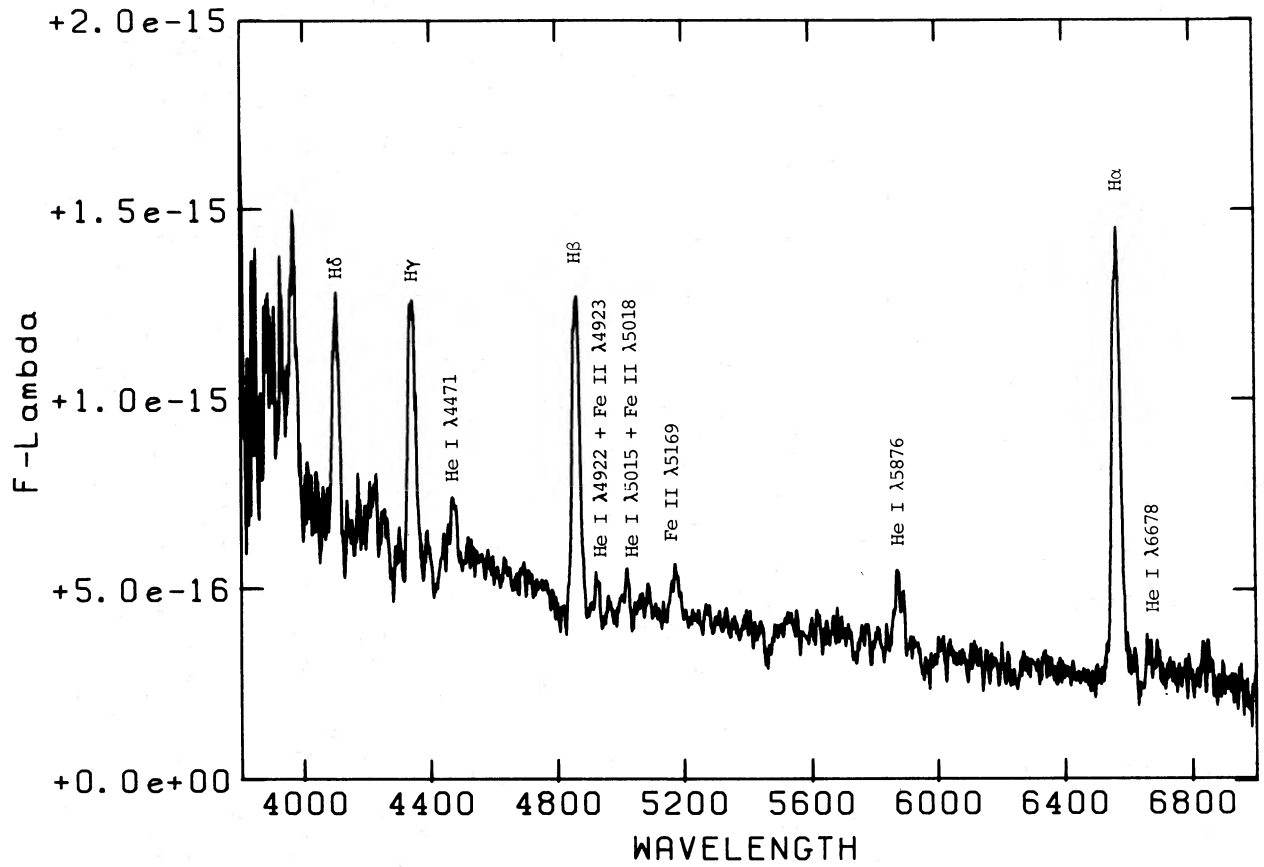

FIG. 1.—The absolute flux of SW UMa (ergs cm^{-2} s^{-1} $Å^{-1}$) is plotted as a function of wavelength. Note the strong emission lines of hydrogen and He I typical of ultrashort-period systems. The absence of He II emission is surprising in view of the fact that SW UMa appears to be a DQ Her system. There is marginal evidence for broad absorption wings at Hβ and Hγ.

neously with *EXOSAT* observations to insure proper phasing between the X-ray and optical observations.

b) *Photometry*

Our optical, high-speed photometric observations were obtained at KPNO. A 2 hr run was obtained on 1983 February 15 UT using the Mk II photometer at the Cassegrain focus of the 1.3 m telescope. The integrations were 10 s in length taken through a *U* filter. The statistical uncertainty of these observations is ~0.04 mag. Two other runs were obtained more than a year later, on 1984 March 7 and 8, using the Mk I photometer and the 2.1 m reflector. These observations spanned ~2 hours each night. The integrations were 5 s long and were cycled through *U*, *B*, *V*, and *R* filters. The statistical uncertainty of these observations is better than 0.03 mag. The optical light curves will be discussed in detail in § IV.

c) *X-Ray*

SW UMa was observed with *EXOSAT* on 1985 March 17 UT. A detailed description of *EXOSAT* can be found in Turner *et al.* (1981). The low-energy Channel Multiplier Array (CMA) detector (0.05–2 keV) was used with the 3000 thin lexan filter from 9:41–11:13 UT and 12:54–15:26 UT, thus covering about three orbital cycles. The Al/P filter was switched in place for one orbit from 11:17–12:50 UT. The medium energy (ME) (2–10 keV) detector was used in an offset mode (so that half the array monitored the background) between 8:52–15:33 UT. The software at the *EXOSAT* center was used for the data reduction. The simultaneous optical spectroscopy obtained at McGraw-Hill established that SW UMa was at quiescence ($V \approx 17$) during the *EXOSAT* observations.

The count rates for the low-energy detector were surprisingly large for a $V \approx 17$ mag cataclysmic variable. The mean value for all observations in the lexan filter was 0.020 ± 0.001 counts s^{-1} and the mean for the Al/P filter was 0.0065 ± 0.0015 counts s^{-1}. The source was detected only at the $\sim 2\sigma$ level in the ME (0.14 ± 0.06 counts s^{-1}). The observations in two filters enabled a crude fit to a source spectrum, which gave equivalent fits with a 0.07 keV blackbody or a 0.21 keV thermal bremsstrahlung source, with a column density of 1×10^{20} cm^{-2}. These fits yield fluxes of 3.2×10^{-12} ergs cm^{-2} s^{-1} and 5×10^{-12} ergs cm^{-2} s^{-1} for the blackbody and thermal spectra, respectively. The limit to the ME 2–6 keV flux is less than 7×10^{-12} ergs cm^{-2} s^{-1} for a 10 keV thermal source spectrum. The corresponding X-ray luminosities for a distance, *d*, are 4.8×10^{30} $(d/100\ pc)^2$ ergs s^{-1} for the 0.05–2 keV range and less than 8×10^{29} $(d/100\ pc)^2$ ergs s^{-1} for the ME range.

The X-ray light curve will be discussed in § IV. A summary of all observations can be found in Table 2.

III. THE RADIAL VELOCITY CURVE

Before discussing the optical photometry and X-ray data further, it is important to establish the orbital parameters of the binary. We begin by discussing the Mount Lemmon radial velocity data. The McGraw-Hill data has been analyzed

TABLE 2

SUMMARY OF OBSERVATIONS

HJD (2,440,000+)	Observer	Telescope	Integration Time	Duration (hr)	Spectral Coverage (λ)	Resolution (Å)
			Spectroscopy			
5465 1983 May 11	A. W. S.	Mount Lemmon	4.8 m	0.8	3800–7000	11
5330 1982 Dec 27	A. W. S.	Mount Lemmon	8 m	1.8	5800–7000	4
5376 1983 Feb 11	A. W. S.	Mount Lemmon	8 m	7	5800–7000	4
5377 1983 Feb 12	A. W. S.	Mount Lemmon	8 m	2.1, 0.6	5800–7000	4
5378 1983 Feb 13	A. W. S.	Mount Lemmon	8 m	1.2	5800–7000	4
6140 1985 Mar 16	J. T.	McGraw-Hill	5 m	2.5	5500–7200	5.5
6141 1985 Mar 17	J. T.	McGraw-Hill	5 m	1.8	5500–7200	5.5
			High Speed Photometry			
5380 1983 Feb 15	P. S.	KPNO 1.3 m	10 s	2	*U*	...
5766 1984 Mar 7	P. S.	KPNO 2.1 m	5 s	2	*U*, *B*, *V*, *R*	...
5767 1984 Mar 8	P. S.	KPNO 2.1 m	5 s	2	*U*, *B*, *V*, *R*	...
			X-Ray			
6141 1985 Mar 17	P. S.	*EXOSAT*	30 s	4.0	(0.05–2 keV) (Lexan)	...
6141 1985 Mar 17	P. S.	*EXOSAT*	30 s	1.5	(0.05–2 keV) (Al/P)	...
6141 1985 Mar 17	P. S.	*EXOSAT*	...	6.5	(2–6 keV) (ME)	...

separately for several reasons. To begin with, the time interval between the Mount Lemmon and the McGraw-Hill observations (~2 yr) is far too long to allow phasing the data sets together. Second, there are considerably more spectra in the Mount Lemmon data set. Finally, the signal-to-noise ratio of the Mount Lemmon data is considerably higher than the McGraw-Hill data. In view of these considerations, we decided to determine the orbital elements using the Mount Lemmon data and to then use these elements in conjunction with the McGraw-Hill data to provide the orbital phasing for the *EXOSAT* observations. The reduction of the McGraw-Hill data followed the general procedure outlined below and the results of this analysis will be compared with the Mount Lemmon data near the end of this section.

Radial velocities have been extracted from the Hα emission lines by convolving the data with a template consisting of two Gaussian bandpasses. Specifically, the wavelength of a spectral feature in a spectrum $S(\Lambda)$ is determined by solving the following equation (Schneider and Young 1980):

$$\int S(\Lambda)G(\lambda - \Lambda)d\Lambda = 0 , \quad (1)$$

where

$$G(x) = \exp\left[-(x - a)^2/2\sigma^2\right] - \exp\left[-(x + a)^2/2\sigma^2\right] .$$

The width (σ) and separation (a) of the Gaussians can be adjusted to measure the velocity at any position in the line profile. This technique has been previously described in Shafter (1985*b*).

In general, the measured velocities will depend on the choice of the parameters σ and a. However, as a first step, we will only concern ourselves with the determination of the orbital period. Any periodicity found in the data should be essentially independent of our choices for σ and a. For oversampled data, such as the image dissector scanner data, the value of σ should be approximately one resolution element. After examining several line profiles, we have found that for our initial purpose a reasonable fit to the line wings is obtained by using $a = 15$ Å and $\sigma = 5$ Å (the choice of the value of a will be further justified later).

After extracting the velocities for our 81 individual Mount Lemmon spectra as described above, we have searched the data for periodicities using the form of the periodogram described by Scargle (1982). The results of our computations are shown in Figures 2 and 3. Because we have data from two observing runs separated by more than a month (1982 December and 1983 February) and our longest coverage on an individual run is only 3 days (February 11–13), we are faced with an annoying 1 cycle per 45 day alias problem (see Fig. 3). Fortunately, our coverage in February was sufficient to eliminate a more serious one day alias problem. The most likely orbital period is 0.05681 days, although this exact value is not well determined (The true period may be a few multiples of a 6 s alias on either side of our adopted period of 0.05681 days). We note that this period is slightly favored to the period of 0.05674 days first reported by Shafter (1983). We will adopt $P = 0.05681$ days, in the discussion to follow, keeping in mind that the true period may be slightly different from this value. Fortunately the aliases are so closely spaced (~6 s) that the uncertainty in the period will not hamper our analysis.

We now proceed to estimate the remaining orbital elements. These include the semiamplitude of the emission-line source, K, the systemic velocity, γ, and the time of conjunction of the emission-line source, t_0. Unlike the orbital period, these elements will generally be functions of the parameters a and σ if any phase-dependent asymmetries are present in the emission lines. For a symmetrical line or for an asymmetrical line whose profile is independent of phase, both K_1 and t_0 should be independent of a. However, generally the line profiles are expected to have a phase-dependent asymmetry. Such asymmetries have been seen in several cataclysmic variables and seem to be the rule rather than the exception (e.g., see Shafter

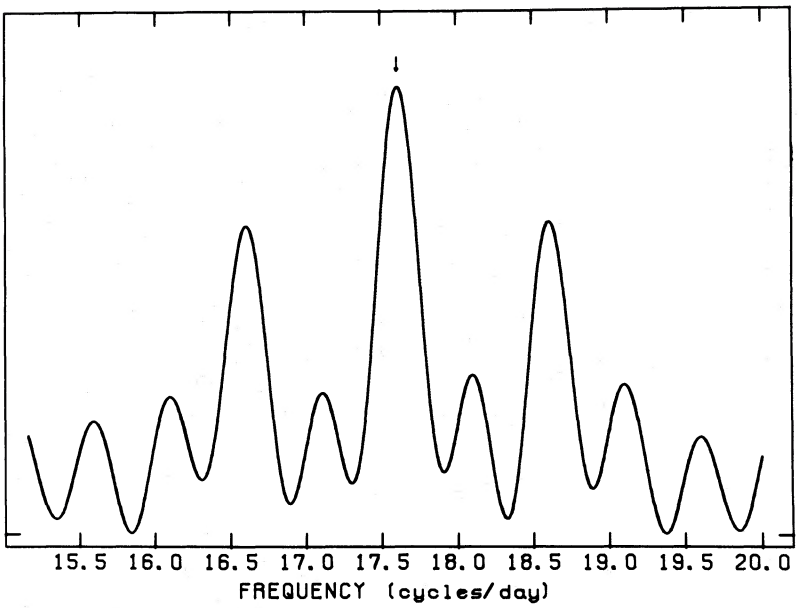

Fig. 2.—The periodogram of our radial velocities of the SW UMa Hα emission line from 1983 February. The orbital period is indicated by the arrow. The ordinate scale is arbitrary.

and Szkody 1984; Schlegel, Honeycutt, and Kaitchuck 1983; Kaitchuck, Honeycutt, and Schlegel 1983). In the majority of cases the asymmetries are attributed to contamination by emission from the vicinity of the hot spot. In this case, the contamination should be concentrated near a velocity which is representative of the projected Keplerian velocity at the outer rim of the disk. If the line is double peaked, then this velocity is approximately given by the half separation of the peaks. Consequently, when attempting to estimate K_1, it is the usual practice to measure the radial velocity variations of the high-velocity emission-line wings which are presumably formed in the inner regions of the disk nearest the white dwarf and farthest from any hot-spot contamination. Nevertheless, in some cases the asymmetry may persist well out into the line wings. For obvious reasons, it is desirable to know the magnitude and extent of any such contamination.

A good way to investigate the extent of any phase-dependent line asymmetries which may be present is to measure the lines using a variety of separations for the Gaussians. In this way the line profile may be "mapped out" in velocity space and any phase-dependent asymmetries may be readily identified. We decided to co-add the data into 10 phase bins before measuring the lines to improve the signal-to-noise ratio in the extreme line wings. The 10 co-added spectra are plotted in Figure 4.

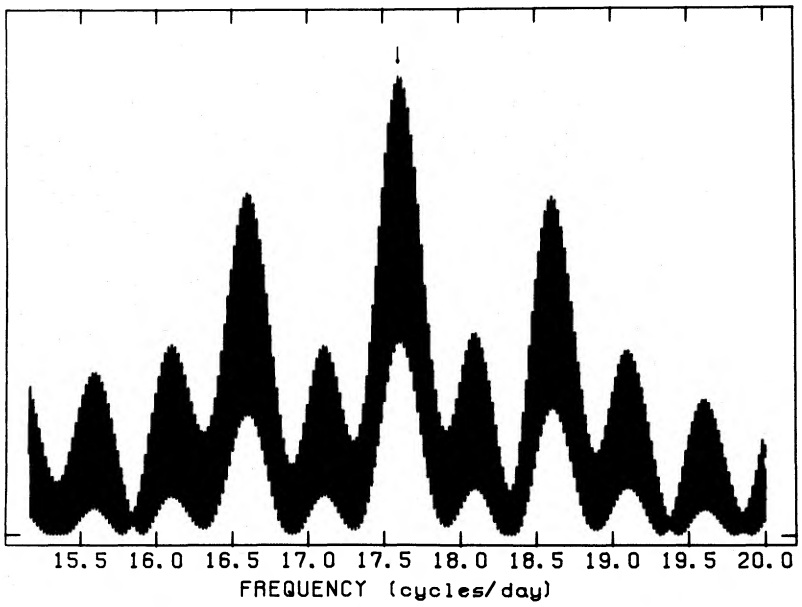

FIG. 3.—The periodogram of our radial velocities of the SW UMa emission line from 1982 December and 1983 February. The adopted orbital period is indicated by the arrow. Note the closely spaced (1 cycle in 45 day) aliases. This spacing corresponds to ~6 s. The ordinate scale is arbitrary.

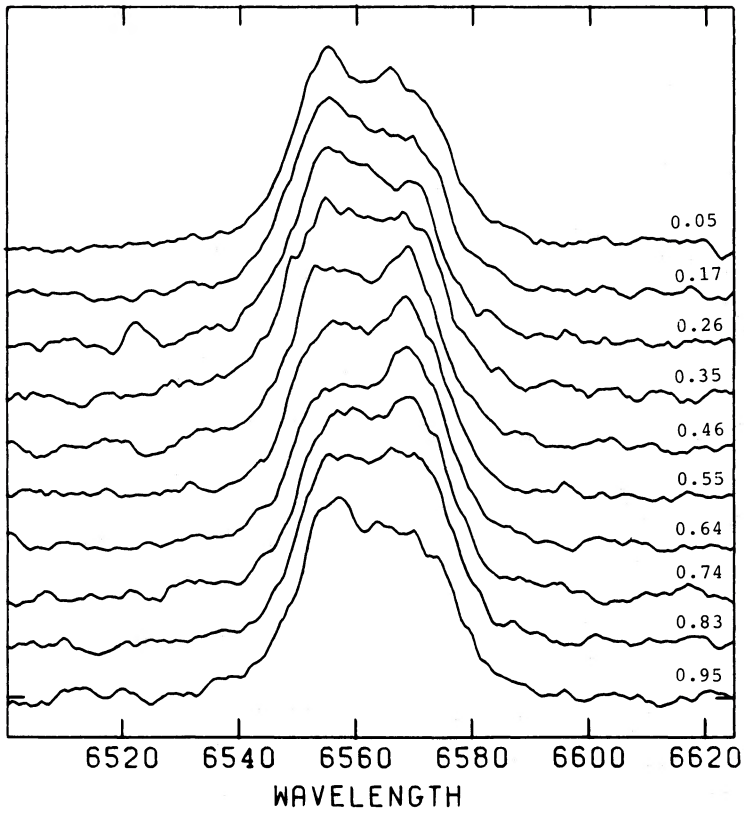

FIG. 4.—The phase-binned Hα emission line profiles on SW UMa from the Mount Lemmon observations. The data have been folded with the 81.8 minute orbital period and summed into 10 orbital phase bins. The orbital phase is given at the right side of the figure. Note the presence of a "s-wave" or peak component which is nearly in phase with the radial velocity variations of the line wings.

In order to determine the orbital elements, we have made nonlinear least-squares fits of the velocity measurements from the 10 phase-binned spectra to sinusoids of the form

$$V(t, a) = \gamma(a) - K_1(a) \sin \{2\pi[t - t_0(a)]/0.05681\} , \quad (2)$$

where γ is the systemic velocity, K_1 is the semiamplitude, and t_0 is the time of conjunction.

It is instructive to plot K_1, its associated error σ_K/K, γ, and t_0 as functions of a. If the asymmetry is confined to relatively low velocities, then the solution for K should asymptotically approach the correct value when a becomes sufficiently large. Furthermore, since the phasing of the perturbing component is not generally expected to be in agreement with the orbital motion, any contamination will usually lead to a spurious phasing in the orbital solution. In this case, we expect that the phasing as measured by the value of t_0 from the orbital solution, will be a function of a. For sufficiently large values of a, then, we can expect the $t_0(a)$ curve to flatten out if the perturbing component is confined to low velocities. Finally, in order to determine the maximum useful value of a, we have plotted σ_K/K. A significant increase in the value of σ_K/K indicates that a has become comparable to the velocity width of the line at the continuum and that the velocity measurements are beginning to be dominated by noise.

Figure 5 shows a plot of K, t_0, γ, and σ_K/K for several values of a. We will refer to this figure as the diagnostic diagram. It is obvious that the Hα emission lines in SW UMa have a phase-dependent asymmetry. In particular, for values of a less than $\sim$12 Å there appears to be contamination by an emission-line component which has the effect of spuriously increasing the

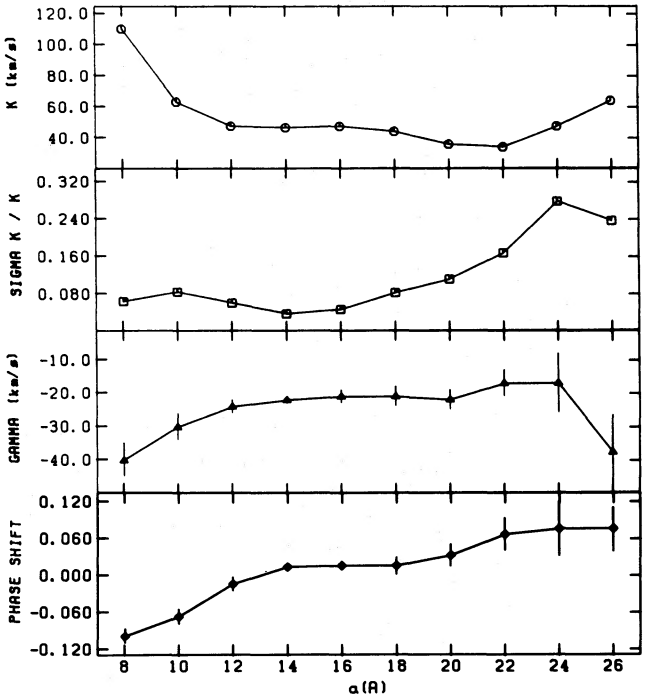

FIG. 5.—The diagnostic diagram for SW UMa. The K-velocity increases when measurements are made near line center. As one measures farther into the line wings the K-velocity converges to a value of 47 km s^{-1} For values of a greater than $\sim$16 Å the velocity measurements begin to be contaminated by noise in the continuum as evidenced by the upturn in the σ_K/K curve.

value of K_1. As the separation of the Gaussians is increased the solution for K_1 appears to converge to a value of 47 km s^{-1}. The fluctuations of K_1 about this value for $a \gtrsim 16$ Å are not significant because the error (σ_K/K) is beginning to rise, indicating that the value of a has become too large. Furthermore, the phase shift decreases and finally disappears for $a \gtrsim 14$ Å. Again, the apparent phase shifts for large values of a are not significant because the Gaussians are no longer sampling a sufficient flux from the emission-line wing. Consequently, we conclude that the best estimate of the semiamplitude of the white dwarf in SW UMa is 47 km s^{-1}. For comparison, the McGraw-Hill data yielded a velocity amplitude of 50 ± 10 km s^{-1}, in excellent agreement with the Mount Lemmon amplitude determined above. The higher K-values obtained by measuring with $a \lesssim 12$ Å is a consequence of contamination by an emission component which is confined closer to the line center. This component can be seen clearly in Figure 4. Henceforth we will refer to it as the "peak component."

The behavior of the peak component is SW UMa resembles that of the s-wave component seen in U Gem except that its radial velocity variations are almost in phase with the motion of the line wings (and presumably the white dwarf). We have estimated the magnitude of the velocity variations of the peak component by directly measuring the wavelength of the line peak by eye. The radial velocity curve derived from measurements of the line wings (base component) is shown in Figure 6*a*. The radial velocity curves for both the peak and base components are shown in Figure 6*b*. Inferior conjunction of the peak component occurs near orbital phase 0.37 (inferior conjunction of the line wings and presumably the white dwarf occurs at orbital phase 0.5 in our phase convention). The fact that both components are almost in phase is surprising. Normally, if the peak component were caused by the hot spot, one would expect that it should be generally out of phase with the line wings instead of being nearly in phase with them. The reason for this is simple. The mass transfer stream should impact the disk somewhere on the side which faces the secondary star. The orbital velocity of material in this region of the disk is generally directed opposite to the velocity of the white dwarf (i.e., $V_d \cdot V_{wd} < 0$). In such a case, one would expect that contamination by the hot spot would have the effect of lowering the K-velocity for measurements made near line center (i.e., for small values of a). The $K(a)$ curve should increase with increasing a until either the hot-spot contamination is gone or until noise in the continuum begins to dominate the velocity measurements. Incidentally, similar behavior would be expected if the perturbing component is generated in the chromosphere of the secondary star.

The behavior described above for a "normal" hot spot is nearly the opposite of what we observe in SW UMa. It appears that the excess emission giving rise to the peak component in SW UMa must be located somewhere on the side of the accretion disk which is *farthest* from the secondary. In addition, the sign of the small phase shift between the peak and base components constrains the region of enhanced emission to be slightly on the *leading* side of the disk. This region of the disk is directly opposite to the impact point of the mass transfer stream. The region of enhanced emission is most favorably observed near orbital phase 0.3–0.4 when the peak component is at inferior conjunction, This is the only location for the origin of the peak component which is able to explain the form of both the $\Delta\phi(a)$ and the $K(a)$ curves (Fig. 5). In the Appendix, we describe line profile simulations which attempt to model the behavior seen in Figure 5 and to specify more precisely the location and extent of the region of enhanced emission.

We now turn to the discussion of the optical and X-ray light curves.

IV. THE LIGHT CURVE

a) Optical

Our optical light curves of SW UMa are shown in Figures 7–9. It is interesting that on two of the three nights (1983 February 15 and 1984 March 8) there appears to be a modulation or "hump" in the light curve. Fortunately, the first photometric run was obtained sufficiently near to our radial velocity observations so that we can estimate the orbital phase of the hump. For the February run, we find that the midpoint of the

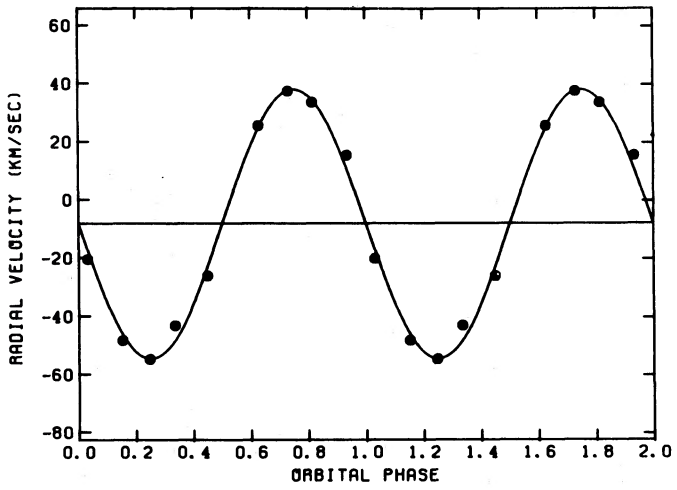

FIG. 6*a*

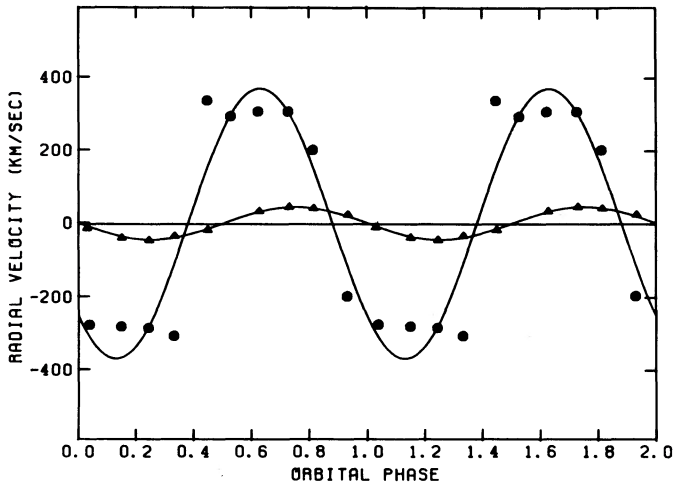

FIG. 6*b*

FIG. 6.—(*a*) The radial velocity curve for SW UMa. The velocities have been measured using a Gaussian separation (2*a*) of 30 Å and represent the motion of the line wings. (*b*) The radial velocity curves for the line wings [same as in (*a*)] and for the peak component of the emission line. Filled circles are the line peak measurements and the triangles are the line wing measurements. Note the fact that the peak and base components are nearly in phase.

hump occurs in the range $0.22 \lesssim \phi \lesssim 0.36$. Because of the alias problem mentioned in § III, the orbital period is not known with sufficient accuracy to enable us to unambiguously constrain the phase of the hump in the 1984 March data. It is worth noting, however, that if we assume that the most likely period is correct then our March data suggests that the hump lies in the range $0.0 \lesssim \phi \lesssim 0.5$. In any case, it is comforting to discover that the phase of the hump maxima seem to be in excellent agreement with the phase of inferior conjunction of the peak component emission determined in the previous section (also see the Appendix). We feel confident that the photometric and spectroscopic data together provide strong evidence that an enhanced source of continuum and line emission arises in the region of the accretion disk illustrated in Figure 14 in the Appendix.

During the reduction of the 1984 March 7 photometry, it became apparent that there was no orbital modulation present, yet there was large amplitude, flickering-like behavior of up to 0.4 mag (peak-to-peak) present on a repetitive time scale of about $\sim$15 minutes. A subsequent Fourier analysis of this nights data revealed a prominent peak at 15.9 minutes (Fig. 10) in all four colors with a pulsed fraction of 5%–8% (tick marks are placed in the *R*-filter plot of Fig. 8 at this period). When the March 8 data were analyzed, a similar period was found with a pulsed fraction of 2%–3%. With only a single orbit covered on each of the two nights (the February 15 data taken with a smaller telescope was too noisy to be useful), it is difficult to definitely assess whether this is a stable feature or merely a characteristic (albeit long) flickering time scale. However, the persistence on two nights suggests a real periodicity, and the X-ray data confirm this interpretation.

b) X-Ray

The low-energy X-ray data were folded with orbital period and averaged in 10 phase bins to increase the signal-to-noise ratio. The absolute phasing was established using the simultaneous McGraw-Hill spectroscopy. The binned data for the two filters are shown in Figures 11 and 12. It is obvious that the X-ray and optical orbital modulations are very similar (Fig. 7). The peak in the X-ray and the optical light occurs near phase 0.3, the same phase as the extra component discovered in the optical spectroscopy (see discussion in § III and the Appendix). The modulation is 50% peak-to-peak in the X-ray light curve, the strength of the flux, and the presence of a 15.9 minute modulation in the optical light curve all point to the possibility that SW UMa is a DQ Her system (Warner 1983; Lamb 1983). Assuming SW UMa is a DQ Her system, we expect a modulation in the X-ray flux at the spin period of the white dwarf. Since the white dwarf should not be phase locked, the spin period is expected to be shorter than the orbital period with the following relationship between the beat, spin, and orbital periods:

$$P_{\rm orb}^{-1} = P_{\rm spin}^{-1} - P_{\rm beat}^{-1} . \quad (3)$$

For SW UMa, we predict that the spin period of the white dwarf is either 15.9 minutes or 13.3 minutes, depending on whether the 15.9 minute optical modulation is the true spin period of the white dwarf or the beat period between a 13.3 minute rotation period and the 81.8 minute orbital period.

In order to search for the X-ray modulation we have folded the 30 s binned Lexan filter X-ray data from 12:54 to 15:26 UT with periods of 13.3 and 15.9 minutes. No modulation was found at the 13.3 minute period. A clear modulation is apparent when the X-ray data is folded with the 15.9 minute period (Fig. 13). Taken together, the X-ray and optical data provide strong evidence for the existence of a magnetic white dwarf which is rotating with a period of 15.9 minutes in the SW UMa system. This conclusion places SW UMa in the DQ Her class of cataclysmic variables.

The general X-ray characteristics of SW UMa are compared to two other DQ Her systems (V1223 Sgr and EX Hya) in Table 3. The excess low energy (0.05–2 keV) flux in SW UMa for its faint optical magnitude is apparent, while the lack of ME flux is consistent with the faint optical magnitude (the ME

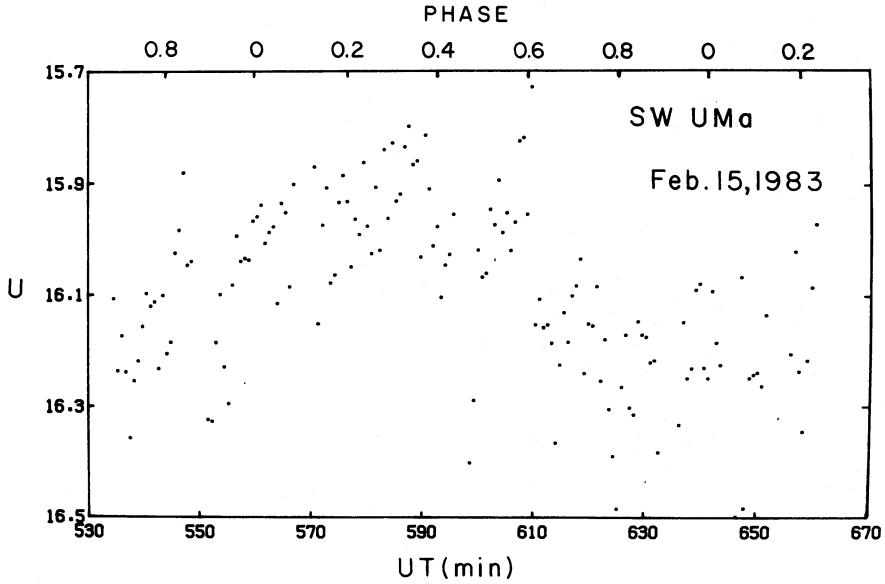

FIG. 7.—The *U*-band light curve of SW UMa from 1983 February 15. Note the sinusoidal modulation at the orbital period. The orbital phase as deduced from the spectroscopy is plotted at the top. It is interesting that the maximum in the light curve occurs at $\phi \approx 0.3$, the same phase where the source of the peak component emission is at inferior conjunction.

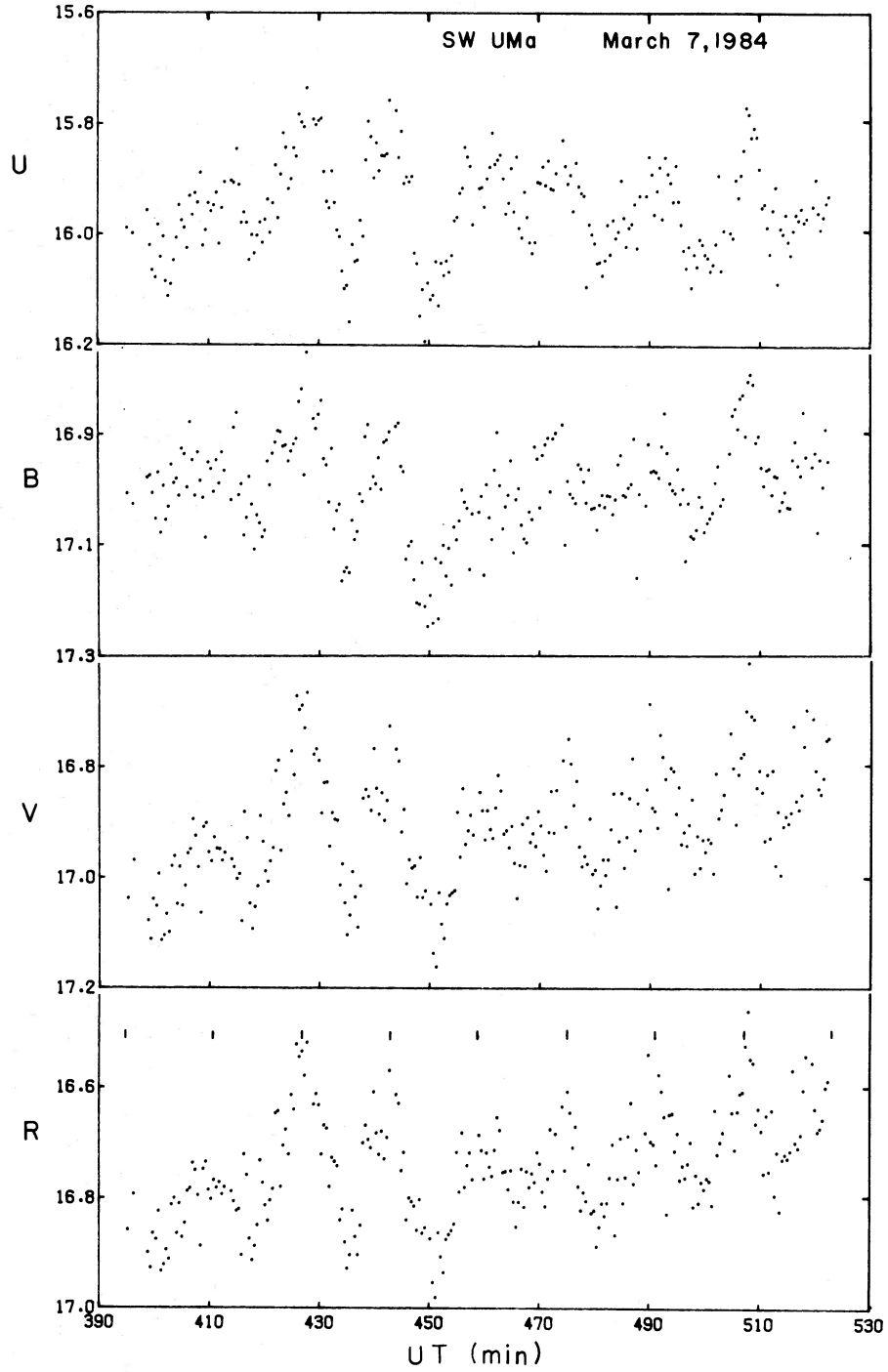

FIG. 8.—The multicolor light curves of SW UMa from 1984 March 7. Note the presence of an apparently stable periodicity in the data at a period of 15.9 minutes. The tick marks in the *R*-band light curve indicate this period.

count rate for V1223 Sgr scaled down by a factor of ~40 to account for the 4 mag difference in the optical flux between these systems is consistent with the lack of detection in the ME). It is interesting that a low-energy blackbody component (0.05–0.4 keV) is also suggested in the V1223 Sgr data (Osborne *et al.* 1984). The lack of strong hard X-rays and He II λ4686 emission in SW UMa argue against a purely magnetic beaming such as in the AM Her systems where the magnetic field inhibits the formation of a disk and the accretion column provides the dominant light. In this configuration, the hard X-ray luminosity is comparable to the soft X-ray blackbody luminosity from the heated white dwarf (Lamb 1983).

The strong soft X-ray flux sometimes observed in cataclysmic variables usually attributed to one of two processes. Either the mass accretion rate is large and the soft X-rays are produced in an optically thick boundary layer (Pringle 1977) or the soft X-rays are produced from radial accretion caused by magnetic channeling in the inner disk (Lamb 1983). We definitely

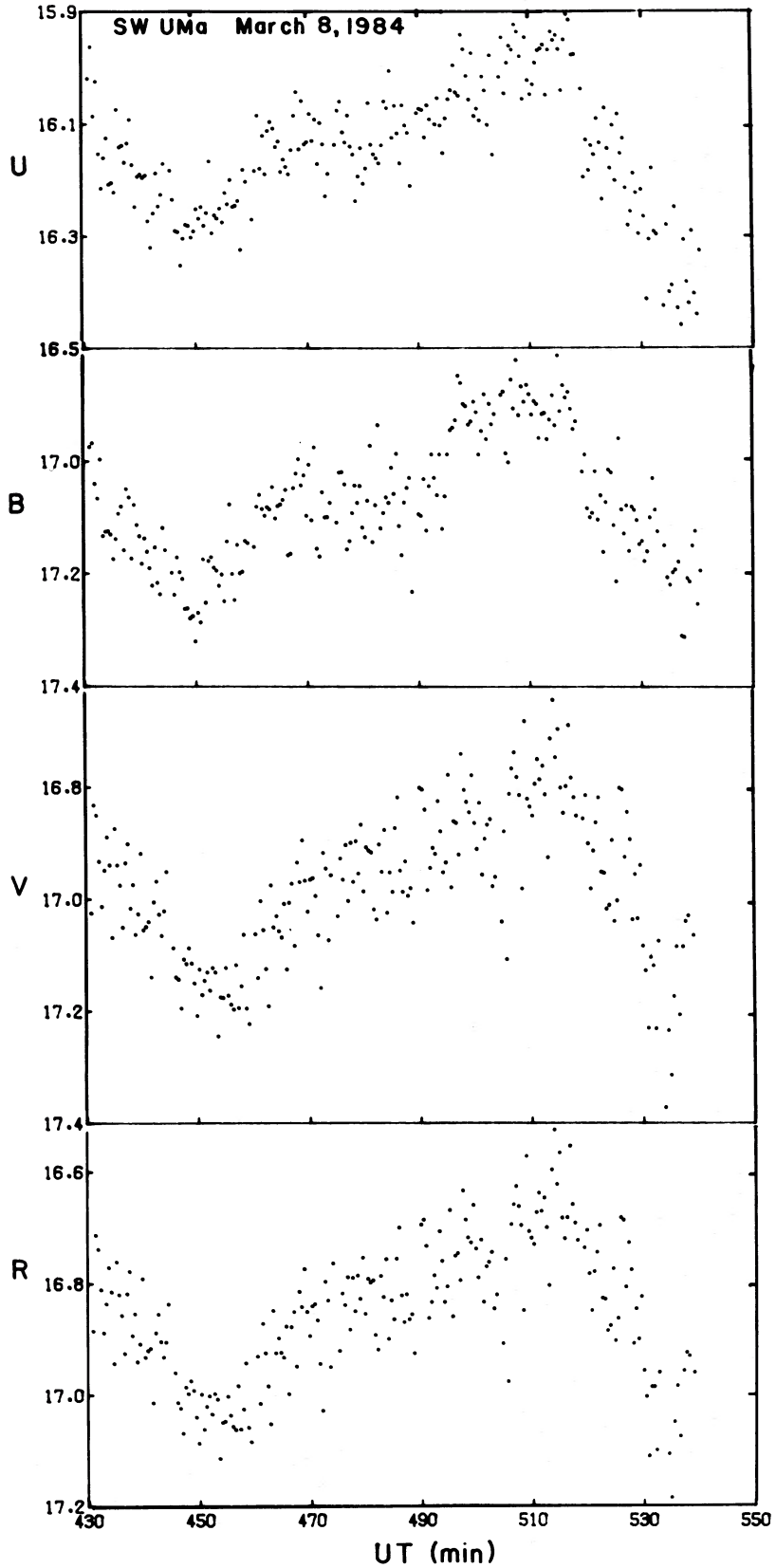

FIG. 9.—Same as Fig. 8 except the data is from 1984 March 8. The 15.9 minute periodicity is not obvious from a visual inspection of the data; however, the periodicity was present in the Fourier transform. The orbital modulation is present in all colors.

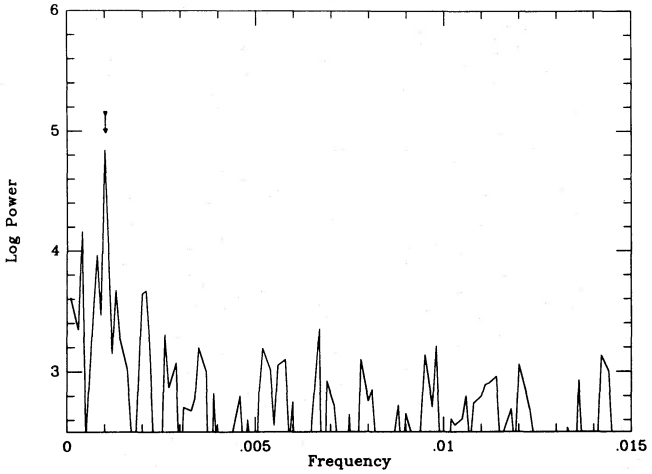

FIG. 10.—The Fourier transform of the 1984 March 7 data. Note the peak at a period of 15.9 minutes.

favor the second interpretation for SW UMa. First of all, the optical spectrum and the short orbital period are not indicative of a high mass-accretion rate. Second, and most importantly, the 15.9 minute optical and X-ray modulations discussed earlier strongly support the conclusion that magnetic accretion is taking place and that SW UMa is in fact a DQ Her system. It is interesting that the dominant optical modulation is at the rotation period of the white dwarf rather than at the reprocessing period. This also appears to be the case in the DQ Her system F0 Aqr (H2215−086) (Cook, Watson, and McHardy 1984). In most other systems the dominant optical modulation is caused by reprocessessing of hard radiation from the magnetic poles of the white dwarf by the secondary star or possibly the hot spot. It is unclear why this does not appear to be the case in SW UMa. Perhaps, the orientation of the magnetic axis of the white dwarf does not intersect a large portion of the secondary or the low mass-transfer rate does not support a well-developed disk with a hot spot at the stream-disk intersection.

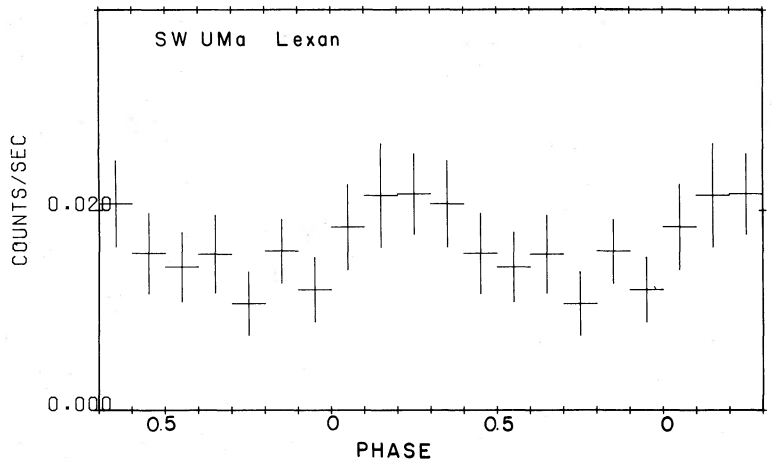

FIG. 11.—The low-energy Lexan-filter X-ray light curve. The orbital phase calibration was made possible by the use of the simultaneous McGraw-Hill spectroscopy. Note that, like the optical observations, the X-ray flux peaks near orbital phase 0.2–0.3.

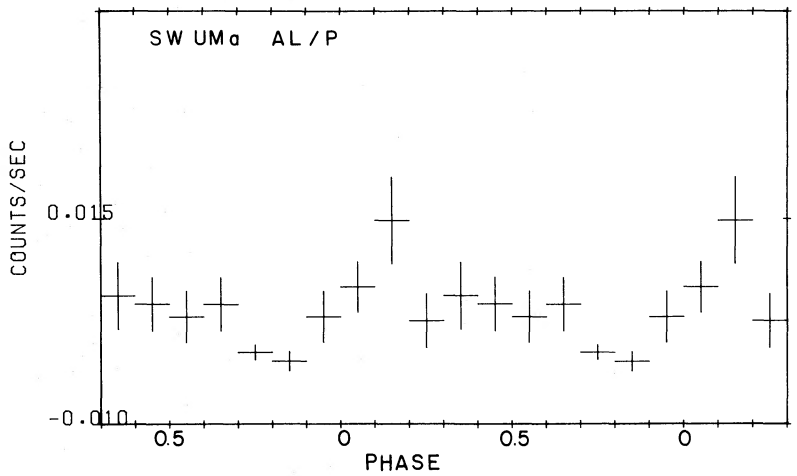

FIG. 12.—Same as Fig. 11 except the Al/P filter was used

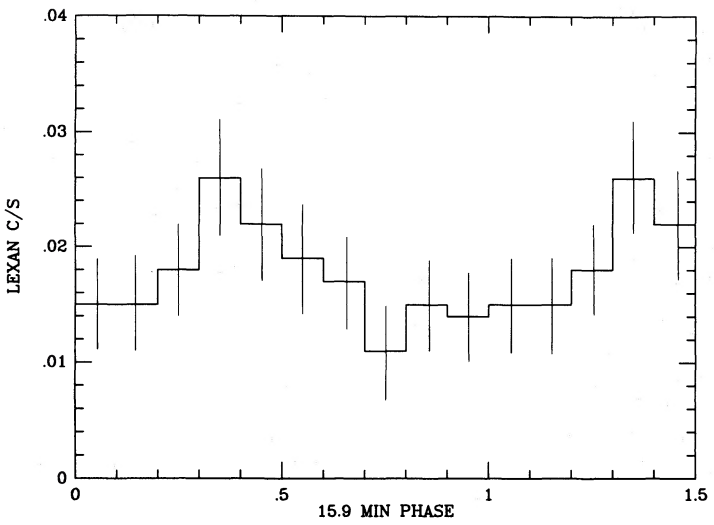

FIG. 13.—The X-ray data (in 30 s bins) has been folded with the 15.9 minute period and plotted as a function of phase. The figure indicates that the X-rays are modulated with the 15.9 minute period.

V. SPECULATIONS, CONCLUSIONS, AND SUMMARY

Although it appears that we have unraveled the basic nature of SW UMa, namely, its identification as a DQ Her system, there are still many unanswered questions. The most glaring of these has to do with the nature of the excess continuum and line emission observed near orbital phase 0.3. Of the two, an explanation for the excess continuum (X-ray and optical) seems less worrisome. It is interesting that the only other DQ Her system with an orbital period below 2 hr (EX Hya) also shows a 0.04–2 keV modulation during the orbital cycle in the same sense as SW UMa—maximum emission at phase 0.3 preceded by a broad depression from phase 0.7–1.0 (Cordova, Mason, and Kahn 1985). This is interpreted as absorption from material in the mass-transfer stream which obscures the X-rays near phase 0.8. This kind of behavior is also reminiscent of other low mass X-ray binaries such as 2A 1822−371 (Mason and Cordova 1982) where the optical and X-ray light curves can be matched with a disk model which has a significant bulge from turbulent thickening where the stream intersects the disk (phase 0.8). The irradiation of this bulge by the X-rays from inside of the disk gives an optical component peaking at phase 0.3 (when the inside of the bulge is viewed from across the disk). This kind of phenomena could be invoked for SW UMa, but the relatively low inclination (lack of eclipses) may present a problem for the required blocking by the stream or disk bulge.

Understanding the origin and phasing of the peak component in the emission line is more difficult. It is hard to imagine how the peak component could be produced in a region of the disk which is effectively opposite to where the hot spot should be formed. One possibility is that material which is heated by the intersection of the mass transfer stream and the disk actually travels a considerable distance downstream before it recombines and gives rise to line emission. This discrepancy between the location of the hot spot and the location of the excess line emission is expected to be greater for the shorter period systems. In the short-period systems the disks are smaller and, for a given white-dwarf mass, the velocity at the outer edge of the disk is higher than for long-period systems. Consequently, in short-period systems, the shocked material not only has a shorter distance to travel to get half way around the disk, it travels faster as well.

In view of its identification as a DQ Her system, it is interesting that SW UMa displays dwarf nova eruptions. If we assume that dwarf nova eruptions are caused by disk instabilities (Meyer and Meyer-Hofmeister 1983; Faulkner, Lin, and Papaloizou 1983; Cannizzo, Ghosh, and Wheeler 1982; Cannizzo and Wheeler 1984; Smak 1984; Mineshige and Osaki 1984), then we can conclude either that the inner disk is not crucial in triggering dwarf nova eruptions, or that the magnetic field in SW UMa does not disrupt a significant fraction of the disk, or both. It seems unlikely that a significant portion of the inner disk is disrupted in SW UMa because our line profile simulations (see Appendix) indicate that the inner disk radius is $\sim 1.5 \times 10^9$ cm. This is a factor of only ~ 1.5 times the radius of a 0.5 $M_\odot$ white dwarf (Hamada and Salpeter 1961).

It is unclear why none of the longer period DQ Her systems, which have larger accretion disks, have been observed to erupt. For a given magnetic field strength, one would expect that a smaller fraction of the disk would be disrupted in these systems, making dwarf novae eruptions more likely than in the shorter period systems. Perhaps the outbursts observed in the ultrashort-period DQ Her systems SW UMa and EX Hya (and possibly other ultrashort-period dwarf novae) are not caused by disk instabilities but rather by an instability in the secondary star (Bath *et al.* 1974; Bath 1985). Consistent with this possibility, Zhang, Robinson, and Nather (1986) have found that the ultrashort-period SU UMa system HT Cas apparently

TABLE 3

COMPARISON OF SW UMA TO SIMILAR DQ HER SYSTEMS

Parameter	SW UMa	V1223 Sgr	EX Hya
V magnitude	17	13	13
Lexan[a]	0.02	0.02	0.3
Al/P[a]	0.0065	0.018	0.1
ME[a]	~0	3.5	7
References	1	2	3

[a] Counts s^{-1}.

REFERENCES.—(1) This work; (2) Osborne *et al.* 1984; (3) Cordova, Mason, and Kahn 1984, Beuermann and Osborne 1984.

harbors a steady state, optically thick disk during quiescence. According to the disk instability modesl, such disks are expected to be stable.

To summarize, we have discovered a 15.9 minute periodicity in both the optical photometry and the X-ray data. We take this as strong evidence that SW UMa is a DQ Her system. In addition to the 15.9 minute periodicity, there is an orbital modulation in the optical and X-ray light curves. The modulation peaks near orbital phase 0.3. In analogy with EX Hya, enhanced continuum emission at this orbital phase may be the result of a better view of the white-dwarf inner disk opposite from the thickened rim of the disk near the hot spot ($\phi \approx 0.8$). Our optical spectroscopy has revealed an excess emission component at Hα. The phasing of this component constrains its origin to the same region of the accretion disk (opposite to the expected location of the hot spot) as the continuum emission. Although difficult to understand, one explanation for the excess line emission is that the disk material which is shocked at the hot spot may travel a significant distance downstream before it cools and recombines producing extra line emission. Using the orbital parameters and system dimensions we have derived for SW UMa, a cooling time of ~ 15 minutes would be necessary if we expect the excess emission component to be most favorably viewed at $\phi \approx 0.3$. Such a long cooling time appears implausible, but without a reliable understanding of the physical conditions in the outer regions of the accretion disk this possibility should not be disregarded.

Several possibilities for future observations immediately come to mind. Further, high-quality, high-speed photometry must be obtained to establish the coherency of the 15.9 minute periodicity and to search for the beat period between the 15.9 minute spin period of the white dwarf and the 81.8 minute orbital period. This beat period should occur at a period of 19.7 minutes. In addition to the photometry, higher resolution spectroscopy would resolve the peak component observed in the Hα line better. Such observations would shed some light on the problem of the origin of this mysterious component.

We thank Rob Robinson for his comments on the original manuscript and Rick Hessman for discussion. P. S. gratefully acknowledges I. Tuohy, A. Parmar, and M. Gottwald for help with *EXOSAT* reductions and the Kitt Peak telescope operators for their help with the optical photometry. This research was partially supported by NSF grants AST-8500790 (A. W. S.) and AST-8405923 (P. S.) and by NASA grant NAG 8-516 (P. S.).

APPENDIX

LINE PROFILE SIMULATIONS

In order to model the behavior of the line-profile variations observed in SW UMa, we have computed synthetic emission-line profiles. The usefulness of these models depends, of course, on the assumption that the magnetic field of the white dwarf only disrupts the inner disk. We assume that a relatively fully developed outer disk exists and that the observed emission line is produced in this residual disk. If dwarf novae eruptions are caused by disk instabilities, then the fact that SW UMa has been observed to erupt implies that the accretion disk is not significantly disrupted.

Our synthetic line profiles are similar to those produced by Stover (1981) in his study of U Gem except that we have included a nonaxisymmetric emission component to model the effect of the peak component identified in § III. Our models are only intended to demonstrate the effect of nonaxisymmetric emission on the amplitudes and phases of radial velocity curves which are derived from measurements of the emission lines. We have assumed that the disk material orbits the white dwarf with the Keplerian velocity appropriate for its radius and that the intensity distribution of the disk follows a modified power law with radius. If i is the orbital inclination, D is the distance to the system, and $R_{\rm in}$ and $R_{\rm out}$ are the inner and outer radii of the disk, respectively, then the line flux at a velocity v from line center is given by the following integration over the disk surface:

$$F(v) = \frac{\cos(i)}{D^2} \int_0^{2\pi} \int_{R_{\rm in}}^{R_{\rm out}} I(r, \phi) G(v, r, \phi) r dr d\phi \,, \tag{A1}$$

where

$$I(r, \phi) = \beta(r, \phi) I_0 (r/R_{\rm in})^{-\alpha} \quad \text{and} \quad G(v, r, \phi) = (2\pi)^{-1/2} s^{-1} \exp\{-[v - v_k(r) \sin(i) \sin(\phi)]^2 (2s^2)^{-1}\} \,.$$

In the above equation $G(v, r, \phi)$ is the local emission line profile from a disk surface element $dS = r dr d\phi$, V_k is the Keplerian velocity at a radius r in the disk, and s is the velocity dispersion of the local line profile. The parameter $\beta(r, \phi)$ defines the form of the disk emission asymmetry. The region of enhanced emission (hereafter REE) is specified by four boundary parameters, $\phi_{\rm min}$, $\phi_{\rm max}$, $r_{\rm min}$, $r_{\rm max}$, and an enhancement factor β. The parameter β is defined to be unity outside the region specified by these boundaries.

Not all of the parameters in equation (3) are independent. For example, the mass of the white dwarf, the orbital inclination, the outer radius of the disk, and the integrated line flux together determine the *scale* but not the *shape* of the line profile. As pointed out by Horne and Marsh (1985), in addition to the scale parameters, there are several parameters controlling the shape of the line profile. These include the ratio of the outer to the inner disk radius which determines the maximum extent of the line wings, the power-law index, α, which determines the shape of the line wings, and the local velocity dispersion, s, which rounds off the double peaks. In addition to the parameters discussed by Horne and Marsh, we must also include the parameter β, which acts as a shape parameter.

Because there are several scale parameters, it is not possible to obtain a unique model for an observed line profile unless additional constraints can be placed on the model parameters. For example, the line width scales as $\sin i$, $M_1^{1/2}$, and $R_{\rm out}^{-1/2}$. A variation in one parameter can be compensated for by the appropriate adjustment of another making a unique combination impossible. If the system were eclipsing, so that the inclination and the outer disk radius could be constrained, then we could produce a unique model. Although SW UMa does not eclipse, we may still be able to constrain parameter space by appealing to indirect arguments.

We begin by introducing two relations which involve the scale parameters. Because the disk material is presumed to be in Keplerian motion around the white dwarf we may write:

$$V_{\rm out} = G^{1/2} M_1^{1/2} R_{\rm out}^{-1/2} \sin(i) \,. \tag{A2}$$

In addition to this constraint, we can make use of the mass function for single-lined systems. If we define $q = M_1/M_2$, then we have

$$M_2 \sin^3 i/(1+q)^2 = 1.22 \times 10^{30} \text{ gm} \,, \tag{A3}$$

where we have adopted $K_1 = 47$ km s^{-1} and $P = 4908$ s. In equation (A2) we may estimate the outer disk radius by assuming that it extends to some fraction f of the primary's Roche lobe. The mean radius of the Roche lobe can be conveniently expressed as a function of the mass ratio of the binary (Paczyński 1971). Specifically,

$$R_1 = 0.462a[q/(1+q)]^{1/3} \,, \qquad q > 2 \,. \tag{A4}$$

This relation, in conjunction with Kepler's third law, enables us to derive the following expression for the outer radius of the disk:

$$R_{\rm out} = 5.5 \times 10^{-4} f P^{2/3} M_1^{1/3} \text{ cm} \,. \tag{A5}$$

The projected velocity at the outer edge of the disk can now be expressed as:

$$V_{\rm out} = 8.18 \times 10^2 f^{1/2} M_1^{1/3} \sin(i) \text{ km s}^{-1} \,, \tag{A6}$$

where M_1 is in solar units and we have used $P = 4908$ s for SW UMa.

For a given value of the secondary mass, equation (A3) enables us to compute the inclination as a function of the white dwarf mass. Figure 14 shows lines of constant M_2 plotted in the $M_1 - i$ plane. In addition, we have included lines of constant $V_{\rm out}$ as defined by equation (A6). These curves have been computed using $f = 0.9$. The computation of several trial models has shown that $V_{\rm out}$ must be near 400 km s^{-1} in order to achieve a reasonable match to the observed line profile. The dashed curves in Figure 14 bound the range of acceptable values of $V_{\rm out}$. The mass of the secondary star may be constrained by assuming that it obeys the mass-radius relation for the lower main sequence. To first order the mass of the secondary star in a cataclysmic binary is a function of the orbital period only. From equation (7) in Patterson (1984) we find that $M_2 \approx 0.1\ M_\odot$ for a period of 1.36 hr. This value is in agreement with evolutionary calculations for the secondary stars in ultrashort period cataclysmic binaries performed by Paczyński and Sienkewicz (1981). We consider the value of $0.1\ M_\odot$ to be an upper limit because the secondary may have evolved toward a degenerate configuration as described in Paczyński and Sienkiewicz.

Constraints on the orbital inclination also suggest that $M_2 \lesssim 0.1\ M_\odot$. The presence of a double-peaked line profile structure implies that the inclination cannot be arbitrarily low, while the absence of eclipses restricts the inclination to be less than $\sim 60°$. Values of M_2 in excess of $0.1\ M_\odot$ require that $i \lesssim 40°$. This seems hard to reconcile with the double-peaked structure. On the other hand, inclinations approaching 60° not only require an evolved secondary, but also require that the mass of the white dwarf be

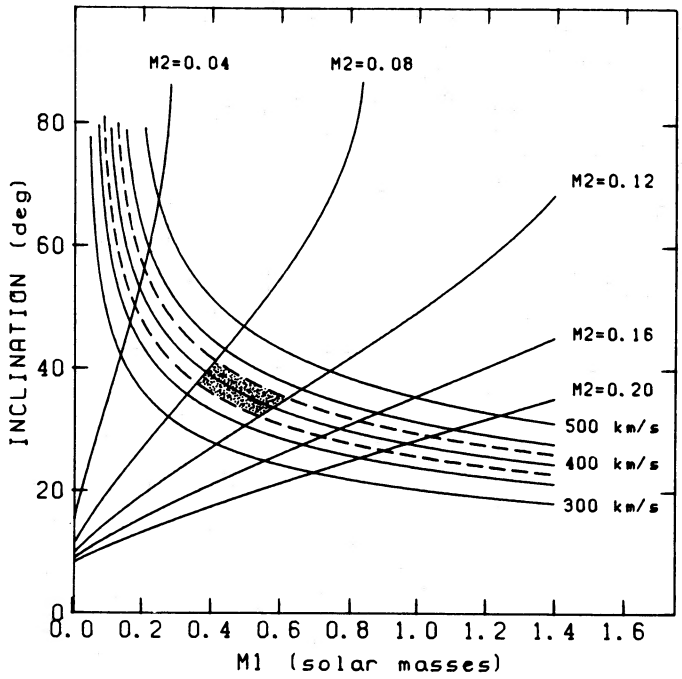

FIG. 14.—Constraints on system parameters for SW UMa. The orbital inclination of SW UMa is plotted as a function of the white-dwarf mass for several values of the mass of the secondary star and for several values of the orbital velocity at the outer edge of the accretion disk. Assuming that the separation of the peaks in the emission line profile approximates the velocity of material at the outer edge of the accretion disk and assuming that the secondary star is near the main sequence, then the most likely location of the SW UMa system is indicated by the shaded region.

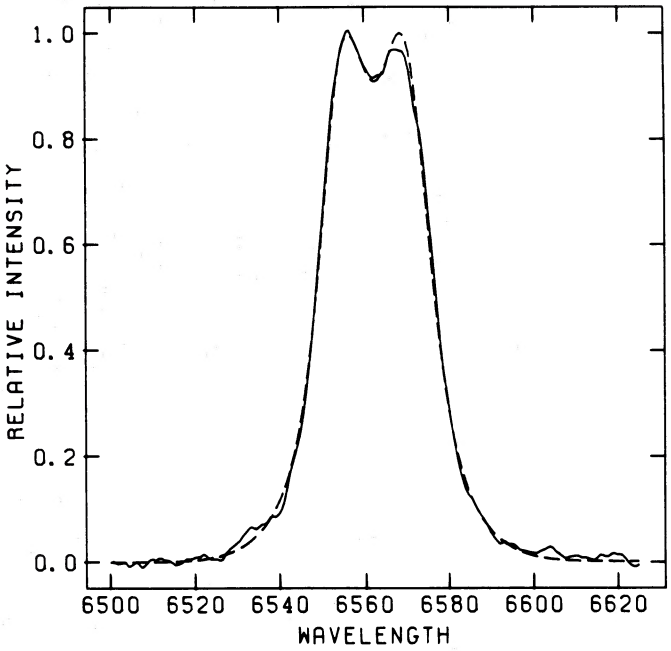

FIG. 15.—Comparison of the mean SW UMa line profile with the best accretion disk line profile model. The parameters for the line-profile model are given in the text.

extremely small ($\sim 0.25\ M_\odot$). Based on the above arguments, it appears that the SW UMa system is most likely located near the shaded region in Figure 14. Consequently, we have adopted $M_1 = 0.5\ M_\odot$ for our model computations. The exact value of the orbital inclination will depend on fits to the observed profile. At this point it is worth remembering that the primary purpose of our line-profile modeling is to simulate the effects of a disk asymmetry on radial velocity measurements, not necessarily to determine accurate masses and dimensions. Our primary objective can be accomplished even if our estimates of the individual scale parameters are poor.

We have computed several sets of synthetic profiles. Each set consists of 10 profiles corresponding to the orbital phases of the 10 binned SW UMa spectra. For each model within a set, the velocity at line center has been computed using the values of K_1, γ, and ϕ determined from the phase-binned SW UMa spectra. Radial velocities have then been determined and $K_1(a)$ and $\sigma(a)$ curves generated for the synthetic spectra using the same technique as for the SW UMa data. Determining the best values for the shape parameters is an iterative procedure. Two requirements must be met simultaneously. First, the brightness and extent of the REE must be chosen so that the synthetic $K_1(a)$ and $\sigma(a)$ curves match the ones for the SW UMa data. Second, the average SW UMa profile must match the average of the synthetic profiles within a set. To meet the second criterion, we have summed the SW UMa spectra into a grand average profile (after correcting for orbital velocity) and have done likewise for the synthetic profiles within a given set.

In order to determine the position and the enhanced emission factor of the REE, we varied the values of $r_{\min}$, $r_{\max}$, $\phi_{\min}$, $\phi_{\max}$, and β until a good match between the observed and the model $K(a)$ and $\sigma(a)$ curves was achieved. After considerable experimentation, we have found that synthetic line profiles computed by using $\alpha = 1.20$, $R_{\rm in} = 1.5 \times 10^9$ cm, $R_{\rm out} = 1.75 \times 10^{10}$ cm, $i = 38°$, $s = 0.23V_k$, $r_{\min} = 0.85R_{\rm out}$, $r_{\max} = R_{\rm out}$, $\phi_{\min} = 210°$, $\phi_{\max} = 270°$, and $\beta = 2.5$ are able to both match the observed profile and to generate $K(a)$ and $\sigma(a)$ curves which match the observed curves reasonably well. The average synthetic profile is compared with the average SW UMa profile in Figure 15. The fit is remarkably good considering the simplicity of the model. To achieve a good fit near

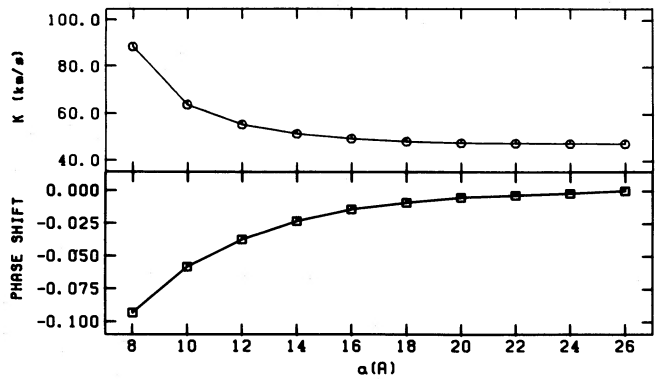

FIG. 16.—The synthetic diagnostic diagram for SW UMa constructed from the accretion disk line profile models. Note the similarity with the diagnostic diagram for SW UMa shown in Fig. 5.

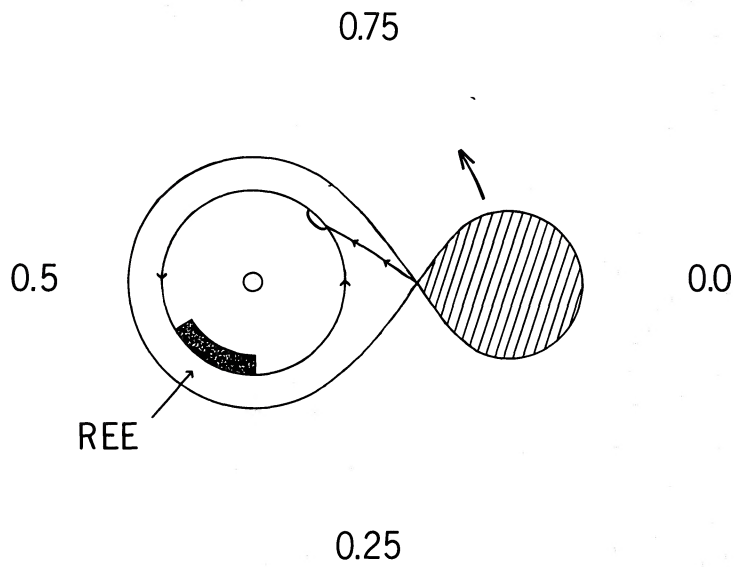

FIG. 17.—A schematic diagram showing the region of enhanced emission (REE) used in the accretion disk line-profile models. The enhanced emission must be located in this general region of the disk in order to produce the observed peak component phasing and to reproduce the observed diagnostic diagram.

line center, we have had to employ a quite large value for the local velocity dispersion (s). A value of $s = 0.23V_k$ indicates that the disk is very turbulent; such a large value may be physically unreasonable. However, for our purposes the important point is that the model profile closely matches the observed profile. The synthetic $K(a)$ and $\Delta\phi(a)$ curves are shown in Figure 16. The synthetic $K(a)$ and $\Delta\phi(a)$ curves are in good agreement with those derived from the SW UMa observations (Figure 5). The REE defined by the above parameters is shown schematically in Figure 17. As expected, the REE must be located on the side of the disk opposite to the secondary star in order to explain the downward slope of the $K(a)$ curve for small values of a. Furthermore, the REE must be located at $\phi > 180°$ in order to explain the sign of the observed phase shift. Finally, the fact that the $K(a)$ curve rapidly converges to a stable value of 47 km s^{-1} requires that the REE cannot extend far into the disk.

REFERENCES

Bath, G. T. 1985, *Rept. Progr. Phys.*, **48**, 483.
Bath, G. T., Evans, W. D., Papaloizou, J., and Pringle, J. E. 1974, *M.N.R.A.S.*, **169**, 477.
Beuermann, K., and Osborne, J. 1984, 18th ESLAB Symposium.
Cannizzo, J. K., Ghosh, P., and Wheeler, J. C. 1982, *Ap. J. (Letters)*, **260**, L83.
Cannizzo, J. K., and Wheeler, J. C. 1984, *Ap. J. Suppl.*, **55**, 367.
Chiapetti, L., Tanzi, E. G., and Treves, A. 1980, *Space Sci. Rev.*, **27**, 3.
Cook, M. C., Watson, M. G., and McHardy, I. M. 1984, *M.N.R.A.S.*, **210**, 7P.
Cordova, F. A., Mason, K. O., and Kahn, S. M. 1985, *M.N.R.A.S.*, **212**, 447.
Faulkner, J., Lin, D. N. C., and Papaloizou, J. 1983, *M.N.R.A.S.*, **205**, 359.
Hamada, T., and Salpeter, E. E. 1961, *Ap. J.*, **134**, 683.
Horne, K., and Marsh, T. R. 1986, *M.N.R.A.S.*, **218**, 761.
Kaitchuck, R. H., Honeycutt, R. K., and Schlegel, E. M. 1983, *Ap. J.*, **267**, 239.
Lamb, D. Q. 1983, in *Cataclysmic Variables and Related Objects*, ed. M. Livio and G. Shaviv (Dordrecht: Reidel), p. 299.
Liebert, J., and Stockman, H. S. 1985, in *Cataclysmic Variables and Low Mass X-Ray Binaries*, ed. D. Q. Lamb and J. Patterson (Dordrecht: Reidel), p. 151.
Mason, K. O., and Cordova, F. A. 1982, *Ap. J.*, **262**, 253.
Meyer, F., and Meyer-Hofmeister, E. 1983, *Astr. Ap.*, **121**, 29.
Mineshige, S., and Osaki, Y. 1984, *Pub. Astr. Soc. Japan*, **37**, 1.
Osborne, J. P., Beuermann, K., Rosen, R., and Mason, K. O. 1984, 18th ESLAB Symposium.
Paczyński, B. 1971, *Ann. Rev. Astr. Ap.*, **9**, 183.
Paczyński, B. and Sienkiewicz, R. 1981, *Ap. J. (Letters)*, **248**, L27.
Patterson, J. 1984, *Ap. J. Suppl.*, **54**, 443.
Penning, W. R. 1985, *Ap. J.*, **289**, 300.
Pringle, J. E. 1977, *M.N.R.A.S.*, **178**, 195.
Robinson, E. L. 1976, *Ann. Rev. Astr. Ap.*, **14**, 119.
Robinson, L. B., and Wampler, E. J. 1972, *Pub. A.S.P.*, **84**, 161.
Scargle, J. D. 1982, *Ap. J.*, **263**, 835.
Schlegel, E. M., Honeycutt, R. K., and Kaitchuck, R. H. 1983, *Ap. J. Suppl.*, **53**, 397.
Schneider, D. P., and Young, P. J. 1980, *Ap. J.*, **238**, 946.
Shafter, A. W. 1983, *Inf. Bull. Var. Stars*, No. 2377.
———. 1985*a*, *A.J.*, **90**, 643.
———. A. W. 1985*b*, in *Cataclysmic Variables and Low Mass X-Ray Binaries*, ed. D. Q. Lamb and J Patterson (Dordrecht: Reidel), p. 355.
Shafter, A. W., and Szkody, P. 1984, *Ap. J.*, **276**, 305.
Shectman, S. A., and Hiltner, W. A. 1976, *Pub. A.S.P.*, **88**, 960.
Smak, J. 1971, *Acta Astr.*, **21**, 15.
———. 1976, *Acta Astr.*, **26**, 277.
———. 1984, *Acta Astr.*, **34**, 161.
Stover, R. J. 1981, *Ap. J.*, **248**, 684.
Turner, M. 1981, *Space Sci. Rev.*, **30**, 513.
Wade, R. A., and Ward, M. J. 1985, in *Interacting Binary Stars*, ed. J. E. Pringle and R. A. Wade (Cambridge: Cambridge University Press), p. 129.
Warner, B. 1976, in *IAU Symposium 73, The Structure and Evolution of Close Binaries*, ed. P. Eggleton, S. Mitton, and J. Whelan (Dordrecht: Reidel), p. 85.
———. 1982, in *Cataclysmic Variables and Related Objects*, ed. M. Livio and G. Shaviv (Dordrecht: Reidel), p. 155.
Warner, B., and Nather, R. E. 1971, *M.N.R.A.S.*, **152**, 219.
Williams, G. 1983, *Ap. J. Suppl.*, **53**, p. 523.
Zhang, E.-H., Robinson, E. L., and Nather, R. E. 1986, *Ap. J.* **305**, 740.

Note added in proof.—High-speed photometric observations obtained by E. L. Robinson, A. W. Shafter, J. A. Hill, M. A. Wood, and J. A. Mattei during a recent eruption of SW UMa have revealed superhumps with a period of 84.0 minutes. This result places SW UMa in the SU UMa subclass of dwarf novae.

A. W. SHAFTER: Department of Astronomy, University of Texas, Austin, TX 78712

P. SZKODY: Department of Astronomy, University of Washington, Seattle, WA 98195

J. R. THORSTENSEN: Department of Physics and Astronomy, Dartmouth College, Hanover, NH 03755